Probabilistic target definition and planning in patients with prostate cancer

Ferjancic, P.; Heide, U.A. van der; Ménard, C.; Jeraj, R.

Physics in Medicine & Biology

IPEM
Institute of Physics and Engineering in Medicine

PAPER

Probabilistic target definition and planning in patients with prostate cancer

To cite this article: Peter Ferjančič *et al* 2021 *Phys. Med. Biol.* **66** 215011

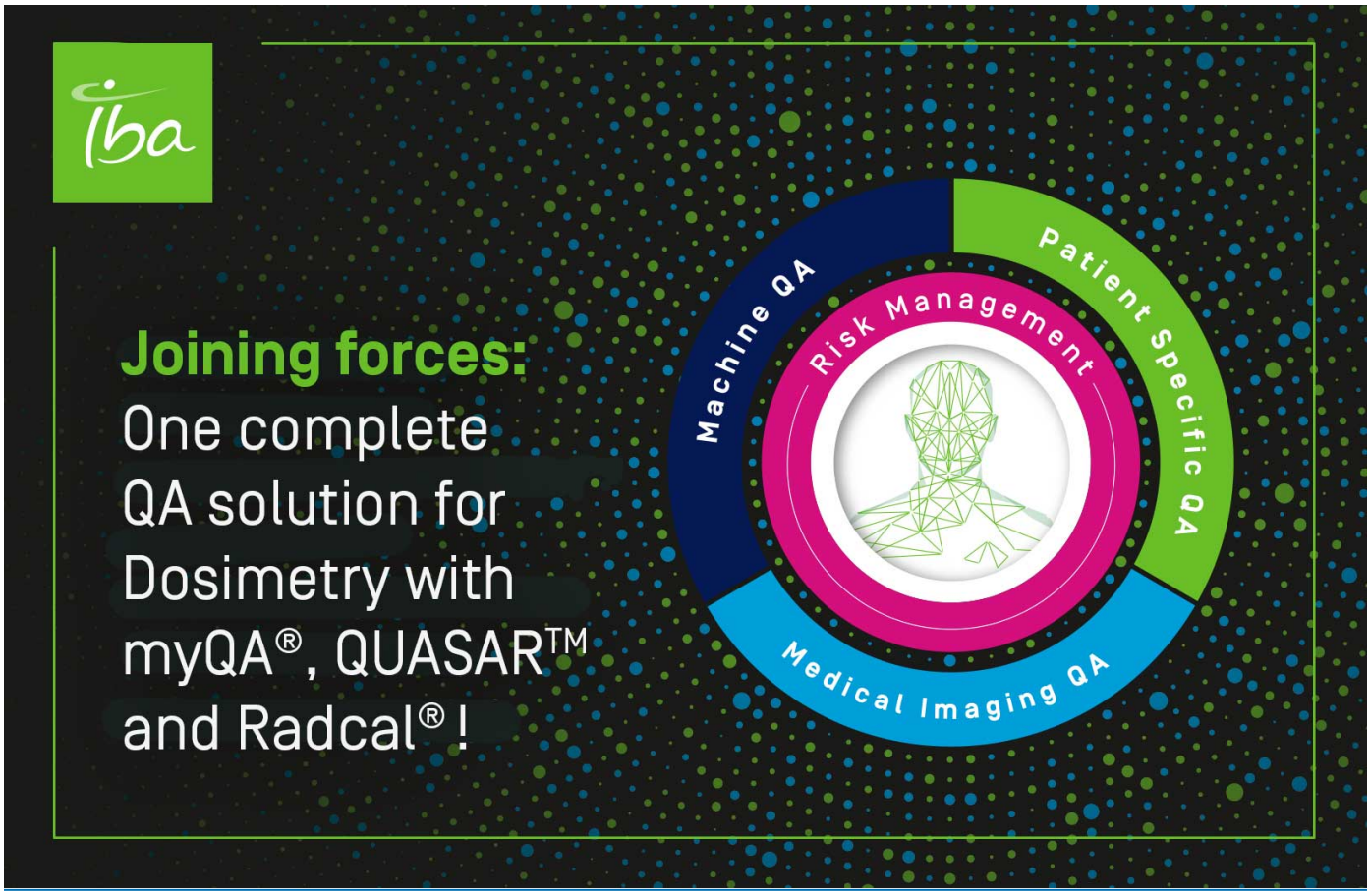

IOP Publishing Phys. Med. Biol. 66 (2021) 215011 https://doi.org/10.1088/1361-6560/ac2f8a

Physics in Medicine & Biology

IPEM Institute of Physics and Engineering in Medicine

RECEIVED
13 July 2021

REVISED
9 October 2021

ACCEPTED FOR PUBLICATION
13 October 2021

PUBLISHED
28 October 2021

PAPER

Probabilistic target definition and planning in patients with prostate cancer

Peter Ferjančič[1], Uulke A van der Heide[2], Cynthia Ménard[3] and Robert Jeraj[1,*]

[1] Department of Medical Physics, Wisconsin Institutes for Medical Research, 1111 Highland Ave, Room 7033, Madison, WI 53705, United States of America
[2] The Netherlands Cancer Institute, The Netherlands
[3] Department of Radiation Oncology, Centre Hospitalier de l'Université de Montréal (CHUM), Canada
[*] Author to whom any correspondence should be addressed.

E-mail: pferjancic@wisc.edu, u.vd.heide@nki.nl, cynthia.menard@umontreal.ca and rjeraj@wisc.edu

Keywords: radiotherapy, probabilistic, prostate

Abstract

Intro. Current radiation therapy (RT) planning guidelines handle uncertainties in RT using geometric margins. This approach is simple to use but oversimplifies complex underlying processes and is cumbersome for non-homogeneous dose prescriptions. In this work, we characterize the performance of a novel probabilistic target definition and planning (PTP) approach, which uses voxel-level tumor likelihood information in treatment plan optimization. *Methods.* We expanded a treatment planning system with probabilistic therapy planning functionality that utilizes non-binary target maps (TM) as voxel-level input to dose plan optimization. Different dose plans were calculated and compared for twelve prostate cancer patients with multiparametric magnetic resonance imaging derived TMs. Dose plans were created using both classical and PTP approaches for uniform and integrated dose boost prescriptions. Dose performance between the different approaches was compared using dose benchmarks on target and organ-at-risk (OAR) volumes. *Results.* Over all dose metrics, PTP was shown to be comparable to classical planning. For plans of uniform dose prescription, the PTP approach created plans within 1 Gy of the classical planning approach across all dose metrics, with no significant differences ($p > 0.2$). For plans with the integrated dose boost, PTP plans exhibited higher dose heterogeneity, but still showed target doses comparable to the classical approach, without increasing doses to OAR. *Conclusion.* In this work we introduce direct incorporation of probabilistic target definition into treatment planning. This treatment planning approach can produce both uniform dose plans and plans with integrated dose boosts that are comparable to ones created using classical dose planning. PTP is a flexible way to optimize external beam radiotherapy, as it is not limited by the use of margins. PTP can produce dose plans equivalent to classical planning, while also allows for greater versatility in dose prescription and direct incorporation of patient target definition uncertainty into treatment planning.

Background

Radiation therapy (RT) planning is subject to intrinsic uncertainties which can affect its results, such as the exact extent of the disease and target positioning. To account for these uncertainties, the International Commission on Radiation Units (ICRU) Report 50, established precise terminology to describe different descriptions of tumor presence using the gross tumor volume (GTV), the clinical target volume (CTV), and the planning target volume (PTV) (Landberg *et al* 1993). While newer ICRU reports 62 and 83 expand on these concepts, additionally adding internal target volume (ITV) they ultimately maintain the same central paradigm (Landberg *et al* 1999, Gregoire *et al* 2010).

Although this approach of expanding volume by margins is pragmatic and historically sensible, it is a simplification of a much more complex process, and it poorly captures the underlying uncertainties. First, delineated volumes can vary considerably depending on the method used or person segmenting (Steenbakkers *et al* 2005, Steenbakkers *et al* 2006, Mercieca *et al* 2018, Aliotta *et al* 2019, Van Herk *et al* 2019). Second, the infiltration of malignant cells into nearby tissues has been shown to be a stochastic process describable with a continuous probabilistic function, rather than a binary delineation (Apisarnthanarax *et al* 2006, Chao *et al* 2006). As such, any description of disease presence is fundamentally probabilistic, a concept which is inadequately captured using simple binary delineations. Previous works have suggested using a probabilistic, or fuzzy logic description of disease presence (Gordon *et al* 2010, Tsang *et al* 2017, Fiorino *et al* 2020, Watkins *et al* 2020), which can better capture the underlying uncertainties. Shusharina *et al* in particular introduced the continuous distribution of voxels to be tumorous as an alternative, probabilistic description of target volume (Shusharina *et al* 2018).

Third, whether the CTV receives the prescribed dose in the presence of uncertainties depends on more than just geometric margins. In reality, the dose distributions are not equally conformal on all sides of the CTV, especially in cases where tumor coverage needs to be balanced against organ at risk (OAR) sparing (Unkelbach *et al* 2018). One alternative way of accounting for uncertainties is robust optimization (RO) (Chu *et al* 2005). RO evaluates the performance of a solution over multiple scenarios in parallel, and was primarily developed to plan intensity modulated proton therapy where the strong nonlinear deposition of dose justifies the higher complexity and computational resources required (Unkelbach *et al* 2008, Fredriksson *et al* 2011, Liu *et al* 2013). With computer power becoming more accessible over the last decade, RO has been increasingly applied to the optimization of external photon beam dose plans (Fredriksson 2012, Unkelbach *et al* 2018).

Fourth, the current treatment planning approach assumes uniform dose distribution to targets—a concept that is intrinsically incompatible with methods of non-uniform dose prescription such as dose painting (Alber *et al* 2003, Bentzen and Gregoire 2011, Jeraj *et al* 2015, Grönlund *et al* 2017). While the effects of heterogeneous dose prescriptions in different disease sites are still being investigated, previous works in prostate cancer, such as the FLAME trial, have shown the benefits of focal lesion ablative boost (Lips *et al* 2011). The results of this trial, conducted on 571 patients, have shown that such boosts can be delivered without an increase in dose toxicity (Draulans *et al* 2020), and with an improvement in biochemical disease free survival (Kerkmeijer *et al* 2021). However, strict dose constraints needed to be followed, compromising the boost dose if necessary. These findings demonstrate the potential benefits of non-uniform dose planning—a well-established concept, but one that is still cumbersome to use when relying on binary target definitions and volume expansion by margins to account for uncertainties (Witte *et al* 2011, Unkelbach *et al* 2018).

The purpose of our study is to develop a probabilistic planning approach for RT treatment optimization and evaluate its feasibility. Unlike in dose painting, this approach modulates the optimization weights using imaging-derived disease information, rather than changing the value of prescribed dose. Probabilistic radiotherapy optimization entices to be an alternative, more flexible way to optimize external beam photon dose plans, as it is not limited by the use of margins and can directly use patient's disease information in treatment plan optimization.

Methods

In this work, we introduce an alternative to the current RT planning workflow: a probabilistic target definition and its incorporation into treatment planning. Rather than using binary disease delineations, we use probabilistic target maps (TM), which assign a probability of disease presence to each voxel within the patient geometry. We implemented this approach within the in-house Tomotherapy planning software, WiscPlan, expanded with RO functionality to account for positioning uncertainties.

We applied the probabilistic target definition and planning (PTP), on a dataset of patients with prostate cancer to validate direct incorporation of imaging-derived disease information into treatment planning and to investigate whether it can create feasible dose plans. Dose plans were calculated using both the classical ICRU approach (using the GTV-CTV-PTV volumes) and the proposed PTP approach using probabilistic TMs. For both planning approaches, a uniform dose plan along with a plan containing an integrated dose boost to the volumes of high disease presence were calculated, resulting in four dose plans per patient. Comparative performance in both uniform and integrated dose boost plans between the two planning approaches were evaluated using dose benchmarks, presented in more detail below.

Patient cohort

Patients with biopsy proven T1–T2 prostate cancer (median age 67, range 54–71 years) were considered for this analysis. The image data for these patients was acquired as part of a previously published investigation (Van

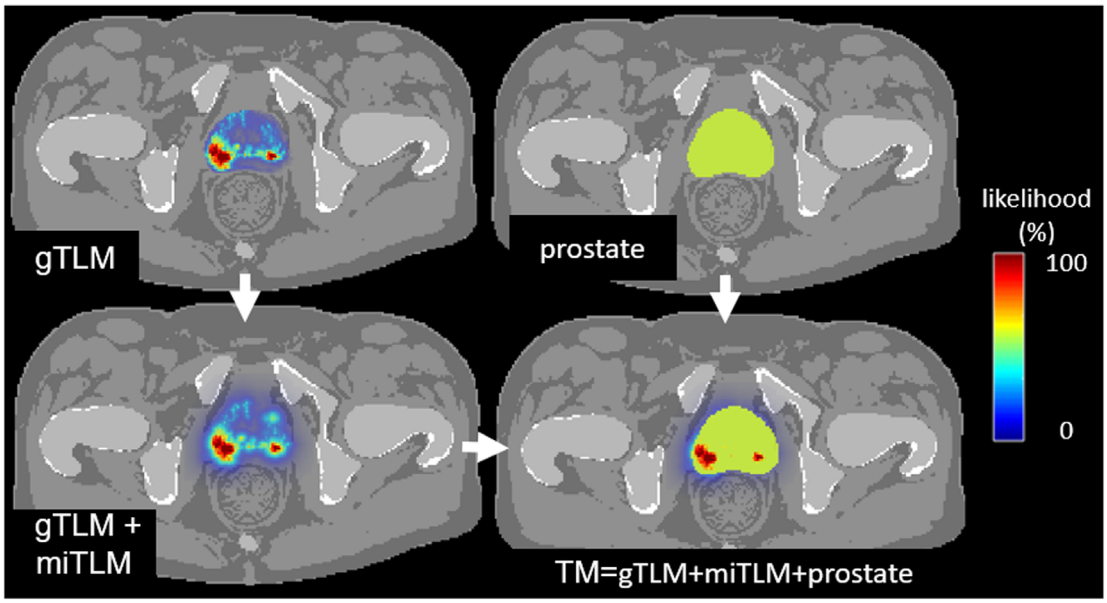

Figure 1. Axial slices of MR-derived CT overlaid with different disease mappings. Top left: initial MP-MRI derived tumor likelihood map (gTLM). Bottom left: gTLM with expected microscopic infiltration (miTLM). Note that unlike gaussian smoothing, this algorithm does not decrease tumor likelihood values within the TLM. Top right: prostate volume. Bottom right: target map (TM) that combines the information of visible and microscopic disease, as well as baseline prostate volume and is used for planning. Areas of high disease presence, and some suspected microscopic extension outside prostate can be seen.

Schie *et al* 2017). Patients underwent multiparametric magnetic resonance imaging (MP-MRI) examinations on a 3.0 T Philips Achieva MR scanner (Philips Healthcare, Best, the Netherlands) at the Netherlands Cancer Institute (NKI). An mDIXON sequence was scanned, from which a pseudo-CT scan was derived using the MRCAT algorithm (Phillips Medical Systems MR Finland Vantaa, Finland). A total of 30 image features from T2w, ADC, and K^{trans} were combined to derive a voxel-level gross tumor likelihood map (gTLM) for the prostate using a logistic regression model (Dinh *et al* 2016, 2017). The study was approved by the ethics committee of the Netherlands Cancer Institute, and patients provided written informed consent.

Planning volumes

Planning volumes were created based on imaging-derived patient data. To account for microscopic disease infiltration, MP-MRI-derived gTLMs were expanded using a sequential probabilistic region growing algorithm (Koritnik 2019) to obtain microscopic tumor likelihood maps (miTLM). The range of infiltration parameter was set to 3 mm, based on existing histological studies evaluating range of extracapsular infiltration (Apisarnthanarax *et al* 2006). To compensate for the low sensitivity of MP-MRI (Lee *et al* 2018, Johnson *et al* 2019, Houdt *et al* 2020), a TM was created by additionally setting the value within the prostate volume to 0.7 to ensure sufficient coverage within the entire prostate gland. This TM creation process of can be seen for an example patient in figure 1.

These TM were used directly in the optimization for PTP planning as described by equations (3)–(5). For the classical approach, the CTV was defined as the volume, where TM probabilities were greater than 0.30, and the PTV was defined as a 4 mm isometric expansion around the CTV.

For integrated dose boost plans, gTLM were first smoothed using a 3 mm gaussian filter to obtain 'TM_{boost}', as seen in figure 2. As each tomotherapy multileaf collimator corresponds to a beam width of just over 6 mm at isocenter, this smoothing reduced the spatial variation observed in the MRI to a level comparable to the resolution of a treatment delivery system, while still being fine enough to retain target sub-volume heterogeneity. For the PTP boost plans, TM_{boost} were used directly as described by equations (3)–(5). For the classical approach, GTV were created using a TM_{boost} threshold of $p > 0.30$, followed by a 4 mm expansion to account for positioning uncertainties. An example representation of all planning volumes can be viewed in figure 3.

Dose prescription and parameterization

Four different dose plans were calculated for each patient, to compare classical and PTP planning approaches in uniform and integrated dose boost prescriptions.

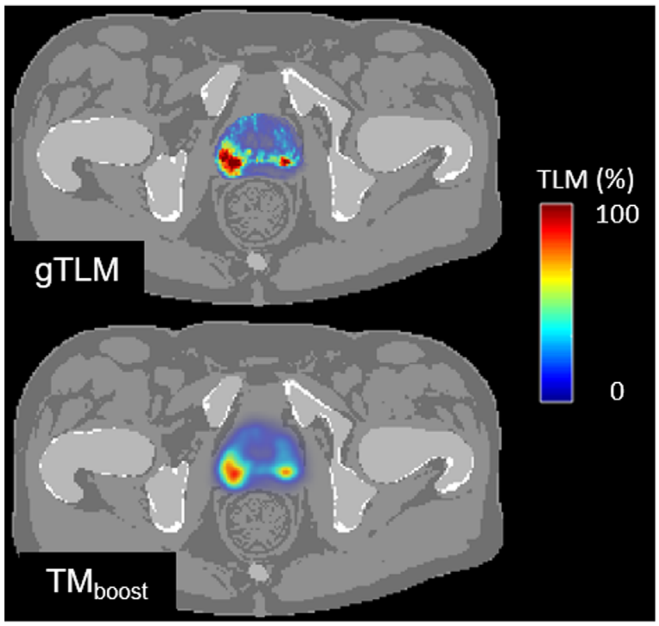

Figure 2. Axial slices of target map used for dose boosting (TM$_{boost}$). In this case, target volume was smoothed using a gaussian filter reduce the spatial variation observed in the MRI to a level comparable to the resolution of a treatment delivery system, while still being fine enough to retain target sub-volume heterogeneity.

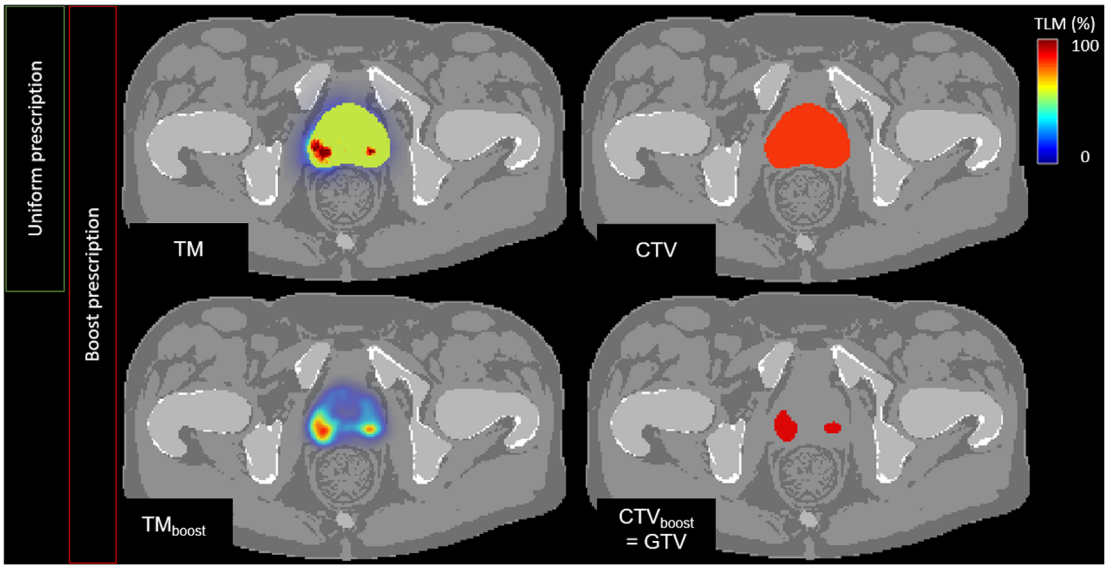

Figure 3. Comparison of probabilistic target volume (TM and TM$_{boost}$) and their analogous classical volumes (CTV and CTV$_{boost}$/GTV) for the example patient.

The first plan was a '*classical uniform*' approach where a dose of 77 Gy was prescribed to the PTV. We aimed at limiting the dose to the rectum and bladder so that the maximum dose to both organs was below 77 Gy. An additional 'soft' objective was added to try and minimize the dose to these organs with a comparatively small optimization weight compared to the other objectives. The optimization function *f(x)* used for this approach was of the general form:

$$f(x) = \sum_{j=1}^{N} (w_j \cdot f_j(q,\, d(x))) \tag{1}$$

for:

$$0 \leqslant x \leqslant mf \cdot \bar{x}, \tag{2}$$

where j is an optimization objective index, w_j is the optimization weight for objective j, f_j is the objective penalty function, q is the prescription objective, $d(x)$ is the dose calculated for beamlet weights x, and mf is the modulation factor.

The second optimization plan was a '*PTP uniform*' approach, where the same dose of 77 Gy was prescribed to the entire volume of the prostate and the seminal vesicles, however in this case the prescriptions were voxel weighted by the TM values as shown in equations (3)–(5). Uniform penalty functions were used for maximum dose prescription as shown in equation (6). Unlike for the minimum dose, the maximum dose needs to be enforced in the entire volume, regardless of likelihood of disease presence.

The uncertainties in patient positioning and dose delivery were accounted for using an objective-based minimax approach in optimization over scenarios of patient misplacement of 4 mm, equal to the PTV margins used in the first plan

$$f(x) = \sum_{j=1}^{N} (w_j \cdot \max\{f_j(q, d(x, s))\}) \tag{3}$$

for:

$$0 \leqslant x \leqslant mf \cdot \bar{x}\,, \tag{4}$$

$$f_{j0}(q, d(x, s)) = \sum_{i=1}^{Ni} (TM(i)) \cdot (\min(D_i, D_{ref,j0}) - D_{ref,j0})^2\,, \tag{5}$$

$$f_{j'0}(q, d(x, s)) = \sum_{i=1}^{Ni} (D_{ref,j0} - \min(D_i, D_{ref,j0}))^2\,. \tag{6}$$

Apart from variables introduced in equations (1) and (2), the s represents scenarios considered, $TM(i)$ represents the likelihood of disease presence in voxel i, D_i is the achieved dose to that voxel and D_{ref} is the prescribed dose in that voxel. Dose constraints to the OAR were kept equivalent to the first planning approach.

The third optimization plan was a '*Classical boost*' approach. This plan was identical to the first, classical uniform approach, except that the maximum dose constraints to the CTV were lessened, and the desired dose within the GTV was set to 95 Gy, as in the FLAME trial (Gurney-Champion *et al* 2020).

The fourth optimization plan was a '*PTP boost*' dose plan. Here, we use the 77 Gy baseline from PTP uniform case and add a prescription for 95 Gy integrated dose boost to the entire target volume, using a voxel-level penalty based on the TM_{boost} in each voxel. OAR prescriptions and uncertainties in patient positioning and dose delivery were handled the same way as for 'PTP uniform' plan.

Implementation and dose optimization

Intensity modulated radiation therapy (IMRT) dose plans were calculated using WiscPlan, an in-house treatment planning software for Tomotherapy delivery systems (Prajapati *et al* 2014, Ten Eikelder *et al* 2020). Dose was calculated for helical deliveries using 64 binary multileaf collimators, 51 angles for the x-ray source position per rotation, a pitch of 0.86 and a 2.5 cm jaw width (Flynn *et al* 2008). Dose calculation was excluded for beamlets that did not intersect the CTV expanded by 4 mm (the classical PTV), and the weights corresponding to those beamlets were omitted in calculations to keep computational burden within machine capabilities.

The classical planning was performed using the existing WiscPlan treatment planning software (Prajapati *et al* 2014). For PTP, the treatment planning software was expanded with probabilistic RO functionality for setup uncertainties, using an objective-level minimax optimization (Van Der Voort *et al* 2016, Ten Eikelder *et al* 2020). A 'good practice scenario selection' approach, where six scenarios of positioning shifts along the main axes, along the 'nominal' scenario using unchanged geometry were used. While the use of higher number of scenarios selected via statistically sound methods may improve robustness of results (Sterpin *et al* 2021), a simpler method had to be used in our work due to limitations of computational resources. To find the function minimum, the constrained nonlinear multivariable function minimum search (*fmincon*), was used in MATLAB 2018b (The MathWorks, Inc., Natick, MA, United States). All optimizations were performed on a system with a 4-core Intel i5-7500 CPU (3.40 GHz) and 16 GB of RAM.

For all optimizations, a maximum modulation factor of 5 was set, and a static dose cloud approximation was used to reduce the computational requirements and to not introduce additional variability between the two planning approaches.

Equivalent optimization weights were used for plans optimized with the classical and PTP approaches. The optimization process ran until step size decreased below a preset threshold, or for a maximum of 200 iterations.

Table 1. Number of beamlets, size of combined volumes of prostate and suspected microscopic infiltration (prostate volume), and volume with high disease likelihood (GTV).

Patient	Prostate volume (cm^3)	GTV volume (cm^3)
1	67.3	3.6
2	37.2	1.7
3	104.2	5.4
4	27.2	7.2
5	53.4	2.8
6	39.8	5.1
7	52.6	1.3
8	27.1	7.5
9	91.5	5.0
10	113.0	29.6
11	45.9	11.9
12	61.7	11.2

Optimization convergence to a local minimum was observed in all optimizations where the optimization did not already converge within this frame.

Dose plan comparison

Dose plans were first evaluated qualitatively using dose volume histogram clouds (DVHs) and quantitatively using dose benchmarks for four volumes of interest. For the CTV and GTV, we evaluated average dose and 95th and 5th dose percentile (D_{mean}, D_{95} and D_{05}). For bladder and rectum OARs, we evaluated average dose (D_{mean}) and fraction of volume receiving at least 77 Gy (V_{77Gy}).

To compare planning approaches, the dose benchmarks were calculated for each planning approach on the nominal scenario and compared in pairs: classical uniform and PTP uniform plans; and classical boost and PTP boost plans. One-sided paired t-tests were used to test the PTP approach for non-inferiority. The tests were left-sided for OAR, and right sided for target volumes, i.e. testing whether doses to OAR were significantly higher in PTP than in classical planning and whether doses to target volumes were significantly lower in PTP than in classical. Results with p-value of less than 0.05 were considered significant. While multiple tests were performed, we did not use p-value correction for multiple hypothesis testing, as this makes for a more stringent non-inferiority test that is not influenced by the number of metrics evaluated.

Results

Twelve patients were selected for planning, resulting in 48 total dose plans. For each patient, target volume and GTV are shown in table 1. An axial slice of a representative dose plan can be viewed in figure 4 and their DVHs can be viewed in figure 5.

A quantitative overview of different planning approaches can be seen in table 2, and the p-values for statistically significant changes between the different approaches can be seen in table 3. Optimization time strongly depended on geometry size and number of objectives: classically optimized plans typically required between 5 and 20 min to calculate, and PTP required between 30 and 120 min.

For uniform plans, dose differences between the classical and the PTP approach were typically less than 1 Gy across all metrics, with no significant differences observed. OAR doses were typically slightly lower and GTV doses slightly higher in the PTP compared to classical planning.

For classical boost and PTP boost plans, none of the target dose metrics decreased, or OAR metrics increased significantly in PTP when compared to classical planning. Residual differences between PTP and classical planning for plans with integrated dose boosts can be seen in Figure 6. GTV doses were higher in PTP boost planning than in classical planning, with average D_{95} increasing 0.7 Gy, D_{mean} 3.4 and D_{05} increasing by 7.3 Gy. At the same time, D_{mean} to bladder and rectum decreased by 1.5 and 1.7 Gy, respectively. PTP plans did have lower average CTV $D95$ by 0.5 Gy, but CTV D_{mean} and D_{05} were increased by 4.4 and 6.4 Gy, respectively.

Discussion

This work introduces a probabilistic radiotherapy optimization approach using direct implementation of non-binary disease maps in treatment planning, in a way that more realistically represents planning uncertainties.

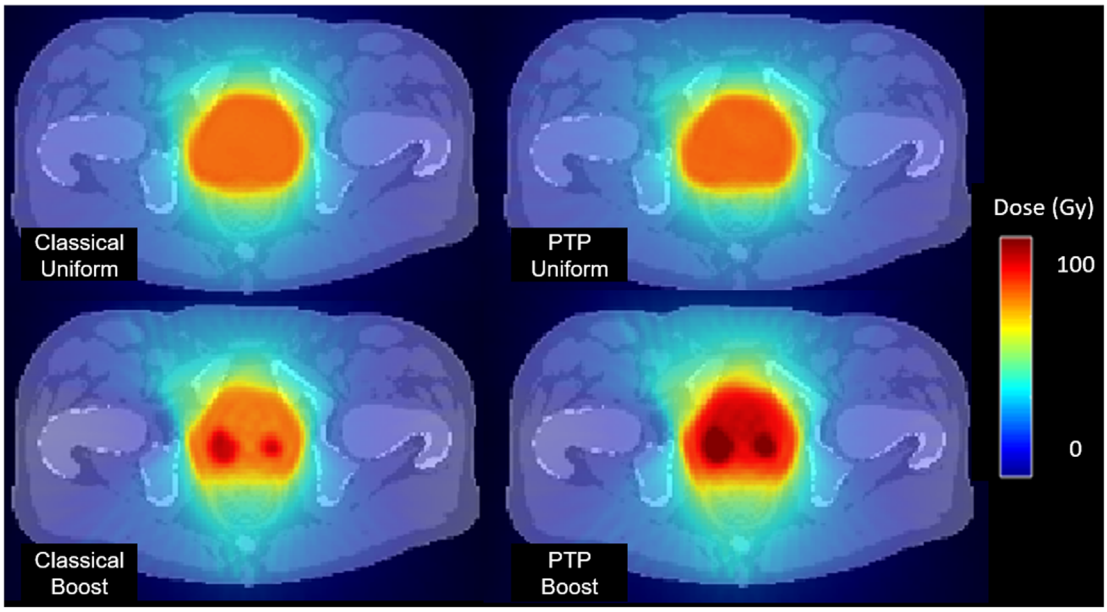

Figure 4. Axial slices of the four different dose plans for the example patient shown in figure 1. Top row shows the classical and PTP uniform plans. The two plans are comparable with very minute differences. Bottom row shows dose plans with integrated dose boosts using the classical and PTP approaches. Here, some differences in dose distributions are observed—most notably higher target doses in PTP approach.

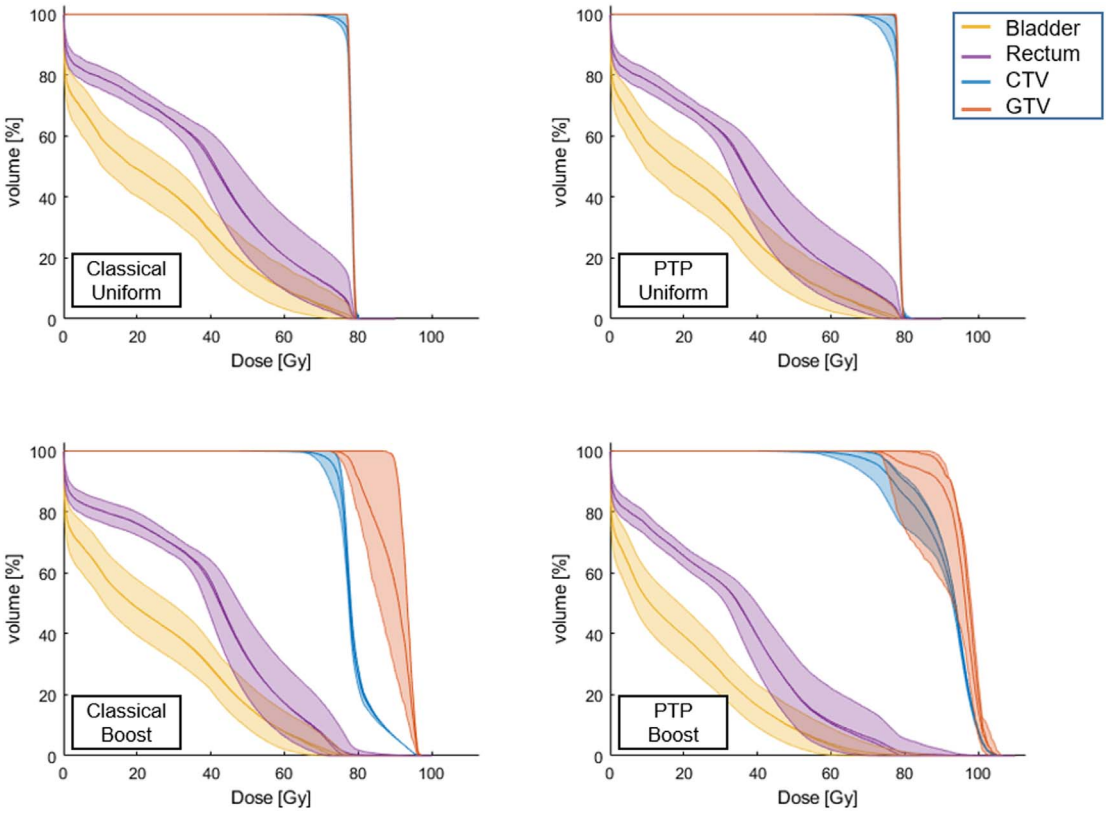

Figure 5. Dose volume histogram clouds of the four planning approaches for the example patient. Histogram bands represent the range of dose performance among all the scenarios considered. This analysis with shifted geometries was performed on classically optimized plans to maintain comparability, even though target expansion by margins was used rather than scenarios of shifts. While PTP tends to generate dose plans with higher target dose heterogeneity, comparable performance is observed for the classical uniform and PTP uniform approaches. For the integrated boost plans, some differences, most notably higher target maximum doses are observed, however the doses to organs at risk does not increase.

Table 2. Average values and their range across scenarios of different realizations of positioning uncertainties for different dose benchmarks considered in the comparison between different dose planning approaches.

	Classical uniform	PTP uniform	Classical boost	PTP boost
CTV D_{95} (Gy)	77 [75.0–78.3]	76.3 [64.4–77.8]	80.3 [75.0–83.4]	79.8 [73.2–84.9]
CTV D_{mean} (Gy)	78.4 [76.1–81.4]	78.3 [74.2–81.0]	87 [79.5–91.9]	91.4 [86.7–94.4]
CTV D_{05} (Gy)	80 [77.4–86.0]	80.2 [79.2–84.8]	94.6 [90.9–95.8]	101 [94.0–107.0]
GTV D_{95} (Gy)	77.1 [75.2–78.4]	77.5 [71.5–80.1]	91.7 [79.2–94.8]	92.4 [87.1–102.0]
GTV D_{mean} (Gy)	78.2 [76.0–81.3]	78.5 [76.5–82.1]	93.9 [89.8–95.3]	97.3 [93.5–105.0]
GTV D_{05} (Gy)	79.4 [76.9–86.0]	79.8 [78.7–84.9]	95.7 [94.6–96.7]	103 [96.0–110.0]
Bladder D_{mean} (Gy)	19.1 [3.51–38.8]	18.4 [3.4–36.6]	18.8 [3.33–35.7]	17.3 [3.34–34.6]
Bladder V_{77Gy} (%)	0.66 [0.00–2.71]	0.60 [0.014–2.64]	0.941 [0.00–3.79]	0.278 [0.00–1.51]
Rectum D_{mean} (Gy)	31.3 [22.6–41.0]	28.9 [21.3–36.6]	31.5 [22.6–41.7]	29.8 [21.2–40.8]
Rectum V_{77Gy} (%)	1.82 [0.00–5.28]	1.26 [0.04–3.66]	2.15 [0.134–4.74]	1.77 [0.00–5.85]

Table 3. Table of *p*-values comparing dose metrics between different plans.

Metric\Plan	Uniform classical v PTP	Boost classical v PTP
CTV D_{95}	1.00	0.97
CTV D_{mean}	0.97	0.72
CTV D_{05}	0.98	0.99
GTV D_{95}	0.91	0.92
GTV D_{mean}	0.28	0.35
GTV D_{05}	0.42	1.00
Bladder D_{mean}	0.63	1.00
Bladder V_{77Gy}	0.88	0.17
Rectum D_{mean}	0.92	0.96
Rectum V_{77Gy}	0.87	1.00

With this approach, both uniform and non-uniform dose distributions can be prescribed and optimized in the presence of uncertainty. With the RO approaches already implemented in some treatment planning systems (e.g. Raystation 4.5), this approach represents a natural evolution that allows a direct implementation of imaging information into treatment planning.

We evaluated the feasibility of this approach on a cohort of patients with prostate cancer. For uniform dose prescriptions, both classical and PTP approaches performed similarly, with no significant differences observed. Identical results were not expected since the two planning approaches are fundamentally different, with different objective functions and optimization algorithms. For plans with integrated dose boosts, PTP resulted in plans with more heterogeneous target dose, but overall, no target doses decreased significantly, and no OAR doses increased significantly. These results show that the PTP approach can achieve dose planning comparable to the classical approach, while allowing greater flexibility in dose planning.

Broadening of the target dose range seems to be a consistent trend with probabilistic planning implementing shift scenarios, as seen in figures 3 and 4, since target optimization goals near OARs tend to compete against OAR limits. In other words, the PTP approach intrinsically trades off target dose optimization objectives for OAR objectives in the presence of uncertainties. While this can raise concerns for underdosing certain target subvolumes, the results of this work showed no significant differences. Additionally, this could be easily adjusted using different optimization functions or objective weights for cases where such underdosing is observed.

This trade-off can also happen within one volume in the presence of multiple competing optimization objectives, such as in the case of integrated dose boost prescribed to the entire CTV volume and weighted using TM_{boost}. This low-weighted pull towards the integrated dose boost prescription allows the dose to breach the non-boosted dose maximum if it results in an overall better dose plan, such as improved target coverage or OAR sparing. This approach can take advantage of previous findings that show that allowing some dose heterogeneity within target volume can lead to sharper dose falloffs and overall better plans (Witte *et al* 2017).

PTP is generalizable beyond the application shown in this work. We chose prostate as our example since existing studies have shown the benefits of focal lesion ablative boost in large-scale clinical trials, but there is no aspect in this approach that prevents its generalization to other disease sites. PTP is also not limited to MP-MRI-derived tumor likelihood maps and can use any imaging modality translatable to TMs, such as positron emission tomography. Additionally, dose prescription is not limited to homogeneous boosts or planning, as the formulation is intrinsically compatible with any dose prescription, such as in dose painting. Lastly, while the

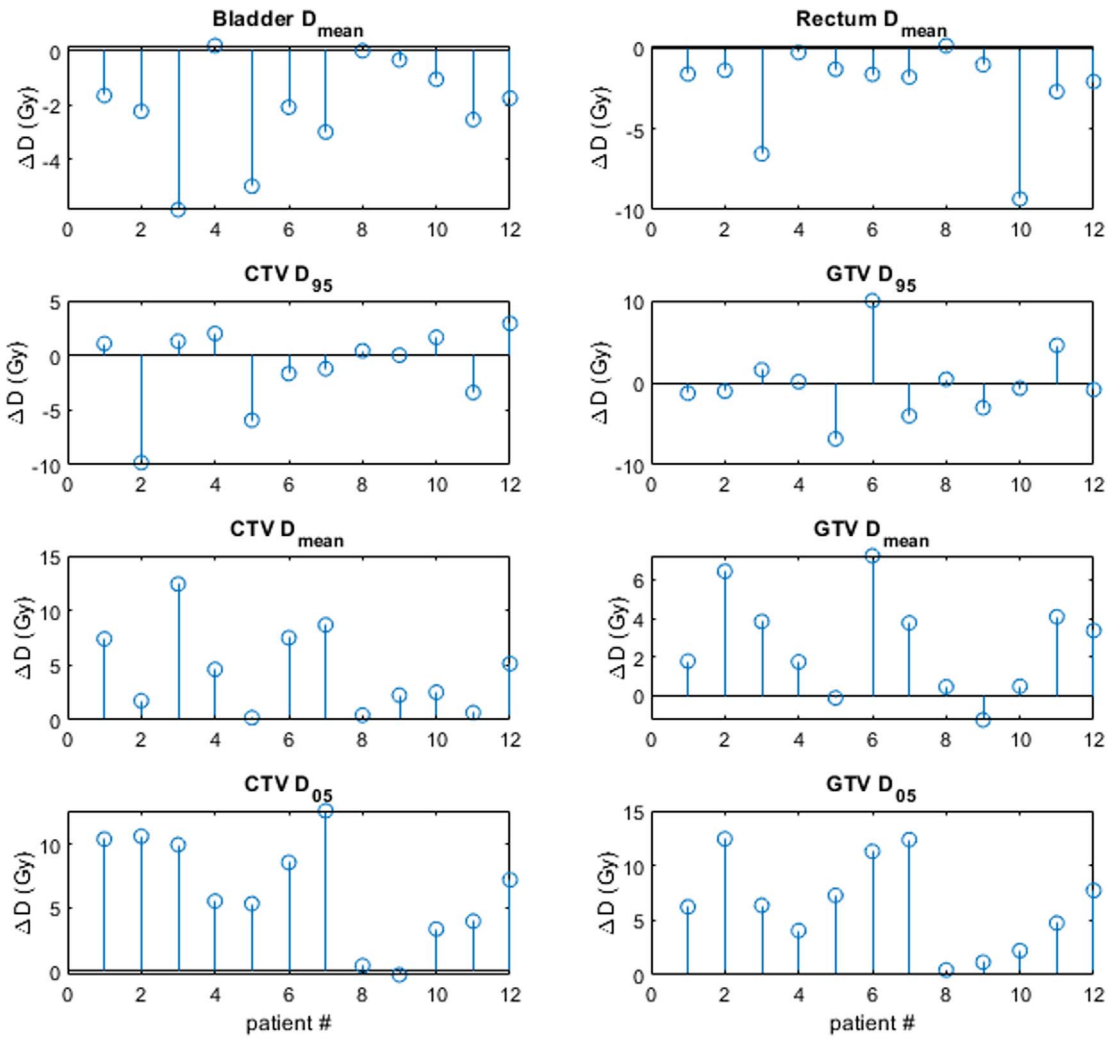

Figure 6. Differences of between PTP and classical planning for all patients and dose benchmarks in plans with integrated dose boost. Values above 0 represent increased, and values below 0 represent decreased doses in PTP, when compared to classical planning. Vertical lines to $y = 0$ are shown to facilitate visual interpretation. PTP plans did not result in increases in OAR or decreases in any of the target dose benchmarks.

implementation of this work was performed using a Tomotherapy treatment planning system, it could be applied in a similar fashion to other systems.

While the approach and main concepts of this work are generalizable, several assumptions were made that limit its scope. First, the initial gTLM maps are subject to considerable uncertainty. The microscopic infiltration algorithm was based on parameters from a single histological study and did not include information regarding anatomic barriers or extracellular matrix that might cause anisotropic cell motility. Additionally, the baseline value of 0.7 for TM within the prostate, and the threshold of 0.3 for the GTV were determined empirically, but as TM values are used as part of overall objective weighting, small variations in this baseline do not substantially affect optimization results. The PTP was not optimized for speed and required considerably longer optimization times. Faster algorithm implementation was considered outside the scope of this paper but could be explored in future work.

While some uncertainty exists in all these input parameters, changing them would not invalidate the general approach introduced in this work. Any improved knowledge of disease presence and uncertainties can still be simply and directly integrated into the PTP approach.

Conclusions

In this work we presented probabilistic target definition and its direct incorporation into treatment planning. We have demonstrated that this probabilistic target definition in combination with known probabilistic optimization produces feasible clinical plans in patients with prostate cancer for both plans of uniform

prescription and plans with integrated dose boosts. Due to its non-reliance on expansion by margins to account for uncertainty, PTP provides a great opportunity to provide more complex dose planning and better use of imaging information to preferentially target subvolumes of increased disease presence.

Acknowledgments

We thank the patients who volunteered their time, and we thank the imaging technologists of NKI who acquired the data. We also thank the members of the ICRU committee for Prescribing, Recording and Reporting Radiation Treatments for their comments and insight.

This work was supported by University of Wisconsin Carbone Cancer Center Support Grant P30 CA014520.

Disclosures

This work was supported by the University of Wisconsin Carbone Cancer Center Support Grant P30 CA014520. Robert Jeraj is the co-founder and CSO of AIQ Solutions. No other potential conflict of interest relevant to this article was reported.

Declarations

Robert Jeraj is the co-founder and CSO of AIQ Solutions.

ORCID iDs

Peter Ferjančič https://orcid.org/0000-0001-9604-9439
Uulke A van der Heide https://orcid.org/0000-0002-4146-6419
Robert Jeraj https://orcid.org/0000-0002-2192-2931

References

Alber M, Paulsen F, Eschmann S M and Machulla H J 2003 On biologically conformal boost dose optimization *Phys. Med. Biol.* **48** 30–5
Aliotta E, Nourzadeh H and Siebers J 2019 Quantifying the dosimetric impact of organ-at-risk delineation variability in head and neck radiation therapy in the context of patient setup uncertainty *Phys. Med. Biol.* **64** 135020
Apisarnthanarax S *et al* 2006 Determining optimal clinical target volume margins in head-and-neck cancer based on microscopic extracapsular extension of metastatic neck nodes *Int. J. Radiat. Oncol. Biol. Phys.* **64** 678–83
Bentzen S M and Gregoire V 2011 Molecular imaging–based dose painting: a novel paradigm for radiation therapy prescription *Semin. Radiat. Oncol.* **21** 101–10
Chao K K *et al* 2006 Clinicopathologic analysis of extracapsular extension in prostate cancer: should the clinical target volume be expanded posterolaterally to account for microscopic extension? *Int. J. Radiat. Oncol. Biol. Phys.* **65** 999–1007
Chu M, Zinchenko Y, Henderson S G and Sharpe M B 2005 Robust optimization for intensity modulated radiation therapy treatment planning under uncertainty *Phys. Med. Biol.* **50** 5463–77
Dinh C V *et al* 2016 Magnetic resonance imaging for prostate cancer radiotherapy *Phys. Med.* **32** 446–51
Dinh C V *et al* 2017 Multicenter validation of prostate tumor localization using multiparametric MRI and prior knowledge *Med. Phys.* **44** 949–61
Draulans C *et al* 2020 Primary endpoint analysis of the multicentre phase II hypo-FLAME trial for intermediate and high risk prostate cancer *Radiother. Oncol.* **147** 92–8
Fiorino C *et al* 2020 Grand challenges for medical physics in radiation oncology *Radiother. Oncol.* **153** 7–14
Flynn R T, Kissick M W, Mehta M P, Olivera G H, Jeraj R and Mackie T R 2008 The impact of linac output variations on dose distributions in helical tomotherapy *Phys. Med. Biol.* **53** 417–30
Fredriksson A 2012 A characterization of robust radiation therapy treatment planning methods-from expected value to worst case optimization *Med. Phys.* **39** 5169–81
Fredriksson A, Forsgren A and Hårdemark B 2011 Minimax optimization for handling range and setup uncertainties in proton therapy *Med. Phys.* **38** 1672–84
Gordon J J, Sayah N, Weiss E and Siebers J V 2010 Coverage optimized planning: probabilistic treatment planning based on dose coverage histogram criteria *Med. Phys.* **37** 550–63
Gregoire V *et al* 2010 ICRU Report 83: prescribing, recording and reporting photon-beam intensity-modulated radiation therapy (IMRT) *J. ICRU* **10** NP.2–NP
Grönlund E, Johansson S, Montelius A and Ahnesjö A 2017 Dose painting by numbers based on retrospectively determined recurrence probabilities *Radiother. Oncol.* **122** 236–41
Gurney-Champion O J *et al* 2020 Quantitative imaging for radiotherapy purposes *Radiother. Oncol.* **146** 66–75
Houdt PP J *et al* 2020 Histopathological features of MRI-invisible regions of prostate cancer lesions *J. Magn. Reson. Imaging* **51** 1235–46
Jeraj R, Bradshaw T, Simoncic U, Simon i U and Simoncic U 2015 Molecular imaging to plan radiotherapy and evaluate its efficacy *J. Nucl. Med.* **56** 1752–65
Johnson D C *et al* 2019 Detection of individual prostate cancer foci via multiparametric magnetic resonance imaging *Eur. Urol.* **75** 712–20

Kerkmeijer L G W *et al* 2021 Focal boost to the intraprostatic tumor in external beam radiotherapy for patients with localized prostate cancer: results from the FLAME randomized phase III trial *J. Clin. Oncol.* **39**

Koritnik A 2019 *Verjetnostna segmentacija tumorjev v področju glave in vratu* University of Ljubljana Phd Thesishttps://repozitorij.uni-lj.si/IzpisGradiva.php?id=112660&lang=eng

Landberg T *et al* 1993 ICRU Report 50: prescribing, recording and reporting photon beam therapy *J. Int. Comm. Radiat. Units Meas.* **os26** NP–NP

Landberg T *et al* 1999 ICRU Report 62: prescribing, recodring and reporting photon beam therapy (supplement to ICRU Report 50) *J. Int. Comm. Radiat. Units Meas.* **os32** NP–NP

Lee M S *et al* 2018 Is prostate imaging reporting and data system version 2 sufficiently discovering clinically significant prostate cancer? Per-lesion radiology-pathology correlation study *Am. J. Roentgenol.* **211** 114–120

Lips I M *et al* 2011 Single blind randomized Phase III trial to investigate the benefit of a focal lesion ablative microboost in prostate cancer (FLAME-trial): study protocol for a randomized controlled trial *Trials* **12** 255

Liu W *et al* 2013 Effectiveness of robust optimization in intensity-modulated proton therapy planning for head and neck cancers *Med. Phys.* **40** 051711

Mercieca S *et al* 2018 Interobserver variability in the delineation of the primary lung cancer and lymph nodes on different four-dimensional computed tomography reconstructions *Radiother. Oncol.* **126** 325–332

Prajapati S, Mackie T R and Jeraj R 2014 Open-source medical devices (OSMD) design of a small animal radiotherapy system *J. Phys.: Conf. Ser.* **489** 012017

Van Schie M A *et al* 2017 Repeatability of dose painting by numbers treatment planning in prostate cancer radiotherapy based on multiparametric magnetic resonance imaging *Phys. Med. Biol.* **62** 5575–88

Shusharina N, Craft D, Chen Y L, Shih H and Bortfeld T 2018 The clinical target distribution: a probabilistic alternative to the clinical target volume *Phys. Med. Biol.* **63** 155001

Steenbakkers R J H M *et al* 2005 Observer variation in target volume delineation of lung cancer related to radiation oncologist-computer interaction: a 'Big Brother' evaluation *Radiother. Oncol.* **77** 182–190

Steenbakkers R J H M *et al* 2006 Reduction of observer variation using matched CT-PET for lung cancer delineation: a three-dimensional analysis *Int. J. Radiat. Oncol. Biol. Phys.* **64** 435–448

Sterpin E, Rivas S T, Van den Heuvel F, George B, Lee J A and Souris K 2021 Development of robustness evaluation strategies for enabling statistically consistent reporting *Phys. Med. Biol.* **66** 045002

Ten Eikelder S C M M, Ferjančič P, Ajdari A, Bortfeld T, den Hertog D and Jeraj R 2020 Optimal treatment plan adaptation using mid-treatment imaging biomarkers *Phys. Med. Biol.* **65** 245011

Tsang H S, Kamerling C P, Ziegenhein P, Nill S and Oelfke U 2017 A novel probabilistic approach to generating PTV with partial voxel contributions *Phys. Med. Biol.* **62** 4917–4928

Unkelbach J *et al* 2018 Robust radiotherapy planning *Phys. Med. Biol.* **63** 22TR02

Unkelbach J, Bortfeld T, Martin B C and Soukup M 2008 Reducing the sensitivity of IMPT treatment plans to setup errors and range uncertainties via probabilistic treatment planning *Med. Phys.* **36** 149–163

Van Herk F B M, Vandaele H V F, De Jaeger S S K and Carbaat N J D C 2019 Inter—observer variation of hippocampus delineation in hippocampal avoidance prophylactic cranial irradiation *Clin. Transl. Oncol.* **21** 178–186

Van Der Voort S, Van De Water S, Perkó Z, Heijmen B, Lathouwers D and Hoogeman M 2016 Robustness recipes for minimax robust optimization in intensity modulated proton therapy for oropharyngeal cancer patients *Int. J. Radiat. Oncol. Biol. Phys.* **95** 163–170

Watkins W T, Nourzadeh H and Siebers J V 2020 Multiobjective, multidelivery optimization for radiation therapy treatment planning *Adv. Radiat. Oncol.* **5** 279–288

Witte M, Shakirin G, Houweling A, Peulen H and Van Herk M 2011 Dealing with geometric uncertainties in dose painting by numbers: introducing the ΔvH *Radiother. Oncol.* **100** 402–406

Witte MM G, Sonke J and Siebers J 2017 Beyond the margin recipe : the probability of correct target dosage and tumor control in the presence of a dose limiting structure Beyond the margin recipe : the probability of correct target dosage and tumor control in the presence of a dose limiting str *Phys. Med. Biol.* **62** 7874–88